Interplay between atomic disorder, lattice swelling and defect energy in ion-irradiation-induced amorphization of SiC

A. Debelle, Alexandre Boulle, A. Chartier, F. Gao, W. J. Weber

Interplay between atomic disorder, lattice swelling and defect energy in ion-irradiation-induced amorphization of SiC

A. Debelle[(a*)], A. Boulle[(b),], A. Chartier[(c)], F. Gao[(d)], W. J. Weber[(e,f)]

[(a)] Centre de Sciences Nucléaires et de Sciences de la Matière, Univ. Paris-Sud, CNRS/IN2P3, 91405 Orsay, France.

[(b)] Science des Procédés Céramiques et Traitements de Surface, CNRS UMR 7315, Centre Européen de la Céramique, 12 rue Atlantis, 87068 Limoges Cedex, France.

[(c)] CEA, DEN, DPC, SCCME, 91191 Gif-Sur-Yvette, France

[(d)] Department of Nuclear Engineering and Radiological Sciences, University of Michigan, Ann Arbor, Michigan 48109, USA

[(e)] Department of Materials Science and Engineering, University of Tennessee, Knoxville, Tennessee 37996, USA

[(f)] Materials Science and Technology Division, Oak Ridge National Laboratory, Oak Ridge, Tennessee 37831, USA

**Corresponding Author: aurelien.debelle@u-psud.fr*

ABSTRACT

A combination of experimental and computational evaluations of disorder level and lattice swelling in ion-irradiated materials is presented. Information obtained from X-ray diffraction experiments is compared to X-ray diffraction data generated using atomic-scale simulations. The proposed methodology, which can be applied to a wide range of crystalline materials, is used to study the amorphization process in irradiated SiC. Results show that this process can be divided into two steps. In the first step, point defects and small defect clusters are produced and generate both large lattice swelling and high elastic energy. In the second step, enhanced coalescence of defects and defect clusters occurs to limit this increase in energy, which rapidly leads to complete amorphization.

I. Introduction

Ion beams are currently used in many fields of materials science and engineering. Two examples are particularly illustrative of their high usefulness: (i) ion implantation, which is a technique that has become an attractive method of controlled doping in many materials, especially in semiconductors [1]; (ii) ion irradiation, which is used as a tool to simulate various radiation environments such as those encountered in nuclear power plants [2]. However, interaction of energetic charged particles with solids has also detrimental effects, the most prejudicial being certainly, in covalent and ionic crystalline solids, the formation of high concentrations of point defects. Two major consequences are atomic disordering, i.e. the loss of long-range and/or short-range order, and swelling of the crystalline structure, both of which affect the physical properties of the material and can lead to loss of structural integrity. Determining the correlation between irradiation-induced defects, atomic disorder and swelling is therefore a topic of utmost importance.

Radiation damage in silicon carbide (SiC), a material envisaged for instance for broad nuclear applications [3] and semiconductor devices [4], has been well studied over the past decades. Indeed, this material exhibits a crystalline-to-amorphous transition, which is accompanied by significant volumetric swelling, under neutron and ion irradiation in the regime where nuclear (i.e. elastic) energy-loss is predominant (see e.g. [3,5-6] and references therein). In this regime, both primary knock-on atoms (PKAs) produced by fast neutrons and incident ions collide with target nuclei, potentially leading to their permanent displacement through direct collisions or via collision cascades [7]. In some materials (e.g. pyrochlores), collision cascades produce point defects only [8], but their accumulation can lead to crystalline-to-crystalline phase transition [9] and even to complete amorphization [9,10]. In several other materials, single collision cascades can produce direct impact amorphization that leads to a complete amorphization by percolation [11]. Depending on the irradiation conditions and on the material, different models of damage

accumulation can be used [12]. In the particular case of the amorphization kinetics in SiC, the 'Direct-Impact/Defect-Stimulated' model is the most employed [6,13-17]. In this model, it is considered that the damage parameter *p* that is used to describe the irradiation damage consists of contributions from both amorphized and damaged-crystalline regions according to the relationship:

$$p = p_a + p_c \quad (1)$$

where p_a is the amorphous contribution and p_c is that of defective (containing point defects and small defect clusters) but still crystalline regions. In this description, p_a is defined as:

$$p_a = 1 - (\sigma_a + \sigma_s) / \left\{ \sigma_s + \sigma_a \exp\left[(\sigma_a + \sigma_s) \Phi \right] \right\} \quad (2)$$

where Φ is the irradiation fluence (or the equivalent dose in dpa). σ_a is the cross-section for direct amorphization, which gives the probability for an amorphous pocket or nucleation site to form inside a single collision cascade, and σ_s is the cross-section for defect-stimulated amorphization, which accounts for the accelerated formation of amorphous clusters presumably due to the presence of defective crystalline regions. p_c is usually reproduced by a simple defect accumulation model, weighted by $(1-p_a)$ [12]:

$$p_c = p_c^{sat} \left[1 - \exp(-B\Phi) \right] (1 - p_a) \quad (3)$$

with p_c^{sat} is the saturation value for the defect-induced disorder, and *B* is an effective recombination volume for the defects giving rise to p_c.

The stimulation of the amorphization process in ion-irradiated SiC has long been observed [6,13-17]. Recently, molecular dynamics (MD) simulations of multiple Si cascades in SiC suggested that this stimulation process is ascribed to an enhanced defect clustering that provides a pathway to lower the energy of the defective SiC lattice [18]. Although in this study the stimulation process was shown to be strongly related to irradiation-induced swelling, the driving force for it to take place remains unclear. In addition, no experiment has been so far undertaken to validate these

predictions. The present paper addresses these issues by combining atomic-level simulations with experimental measurements to correlate atomic disorder, lattice swelling and system energy in ion-irradiated SiC. For this purpose, a methodology is proposed where experimental X-ray diffraction (XRD) patterns and XRD patterns generated using MD calculation cells are similarly processed (yet adapting the theory to the situation), therefore allowing for direct quantitative comparison.

II. Experimental and computational details

II.1. Experiments

In this work, (001)-oriented 3C-SiC single crystals were irradiated with 100 keV Fe^{+} ions at room temperature in the $4x10^{13}$ – $4x10^{14}$ cm^{-2} fluence range [6], which corresponds to damage doses of 0.07 to 0.7 displacements per atom (dpa) at the damage peak, as determined with SRIM calculations [19] using the recommended threshold displacement energies of 20 eV and 35 eV for the C and Si sublattices, respectively [20-21]. The weighted average recoil spectra [22] were calculated from the SRIM data. These plots allow determining the PKA energy $T_{1/2}$ for which half of the defects are created by recoils with a greater energy, and half of the defects are produced by recoils with an energy lesser (than $T_{1/2}$). This characteristic energy provides a reasonable way to compare different irradiation conditions in the nuclear energy-loss regime [22]. Values of ~3.7 keV and ~4.6 keV were found for Si and C PKAs, respectively. High-resolution X-ray diffraction (HRXRD) experiments were carried out at the BM02 beamline of the European Synchrotron Radiation Facility (ESRF, Grenoble, France). The wavelength of the X-ray beam was 0.148787 nm, and the beam divergence, estimated from the peak width of an unirradiated crystal, was ~0.01°. Longitudinal θ-2θ scans were recorded around the (004) reflection of SiC over a range wide enough to include the scattering from the irradiated region, as illustrated in Fig. 1 (thick lines). The

(004) reflection was chosen because it provides the best compromise between scattered intensity and resolution. The experimental curves were simulated (see thin solid lines in Fig. 1) with a procedure that allows the determination of both the lattice strain (homogeneous lattice displacements) and lattice disorder (random atomic displacements) depth profiles in the irradiated region [23,24]. The corresponding strain profiles are provided in the inset of Fig. 1. Hereinafter, only strain and disorder values at the damage peak (i.e. ~30 nm) are discussed. This region is expected to be the most relevant because surface effects and influence of the interface with the pristine crystal are expected to be limited.

II.2. Computer simulations of collision cascades (CC)

MD calculations were performed to simulate collision cascades (CC) induced by 10 keV Si recoils in SiC; cascade overlapping was computed to reproduce damage accumulation up to complete amorphization. The corresponding computational methods were described previously [25]. In that work, calculations were conducted at 200 K. The number of atoms (40 000) contained in the simulation cell was kept constant, but the simulation cell was allowed to expand or shrink along the three directions. In contrast, materials actually irradiated with low energy ions are similar to thin layers fixed on a thick unirradiated crystal (comparable to a substrate) and consequently no in-plane dimensional change is possible [26-28]. For this reason, additional MD calculations have been conducted using simulation cells where in-plane dimensional change was forbidden, see below sect. II.3.

II.3. Frenkel pair accumulation (FPA) simulations

The purpose of the Frenkel pair accumulation calculations was to simulate the amorphization process in SiC considering a crystal (or a cell) where only the out-of-plane direction

was free to accommodate the radiation damage, as it is the case in actual experiments. The FPA method was employed because it is much less time-consuming than CC simulations, and it has been proven to nicely mimic amorphization processes in SiC [29] and in pyrochlores [30]. Briefly, this methodology consists in continuously creating Frenkel pairs in the framework of molecular dynamics calculations [31]. To do so, a silicon atom or a carbon atom is randomly selected and displaced in the super-cell. Calculations are performed at room temperature. The dimensions of the basal planes of the super-cell were kept constant in the present study, inducing the development of in-plane stresses, while the c-axis was stress-free. Note that contrary to the study reported in [29] where only C defects were introduced to reproduce amorphization upon low-energy electron irradiation, in the present work, both C and Si Frenkel pairs were generated, which is more representative of the actual disordering process and kinetics occurring during ion irradiation.

II.4. Methodology for the data processing

The aim of the methodology presented here is to propose an original way to process experimental and computational data for a direct and reliable comparison. For this purpose, the same physical signal was used, which is in the present case an XRD signal; this approach allows avoiding biases that are usually inevitable when using different techniques or methodologies. More precisely, XRD measurements were performed and the corresponding data were compared to atomic-scale information converted into a predicted (XRD) experimental signal. The word “predicted” is here highly important, because it indicates that the methodology does not rely on a specific defect model. It does not serve the purpose to reproduce a set of experimental data, but on the contrary experiments and simulations are carried out separately and the data are then similarly processed. In addition, it provides quantitative results, on both disorder and strain, over a

large dose range. For these reasons, it is different from the innovative approach implemented by Nordlund et al. who computed diffuse scattering intensity to fit experimental grazing-incidence X-ray scattering signal and obtained the size of the stacking faults formed in implanted Si [32]. It also differs from the original work carried out by Li et al in titanate pyrochlore where irradiation-induced swelling determined by XRD was ascribed to cation antisite defect formation thanks to MD calculations of the relaxation volumes of different types of defects [33].

In the present work, to determine disorder and lattice swelling, XRD patterns have been obtained experimentally or generated from the simulation cells. In the former case, the dynamical theory of diffraction was required to rigorously take into account specific scattering effects such as multiple diffraction and extinction which occur in these systems, contrarily to powder, polycrystalline or nanostructured materials. The curves were then, as mentioned in sect. II.1., fitted using the procedure described in [23,24]. In the latter case, the kinematical theory was sufficient due to the nanoscopic structure of the simulation cells. The pair distribution functions (pdf) were computed from the calculated structures and the XRD patterns were obtained by a Fourier transform of these calculated pdf. Then, peaks corresponding to the (004) reflection were fitted with a pseudo-Voigt function that allows to precisely obtain peak integrated-intensity and position. Hence, the theory was adapted to the nature of the object giving rise to the XRD signal. However, and this is worth emphasizing, in both cases, the disorder and the strain were obtained using the same procedure. Disorder was derived from the evaluation of peak intensity lowering through the so-called static Debye-Waller factor [23,24]. This evaluation does not require the usual assumption of normally distributed atomic displacements, which is probably not justified within collision cascades. The lattice swelling was straightforwardly derived from the peak shift using the derivative of Bragg's law.

III. Results and discussion

III.1. Disordering kinetics

As a preamble to this section, it appears necessary to explain how defects are defined and labelled in the following. Based on previous works of MD calculations of collision cascades in SiC [25,34-36], small defect cluster refers to an aggregate of a few (typically 3-4) atoms, while a much larger cluster can be considered as amorphous (based on the criterion of total pair correlation function) when it contains a few tens (typically at least 30) of atoms.

The disordering kinetics derived from XRD measurements was compared to those obtained from the two simulation methods (Fig.2). The three curves appear to be different but this is not surprising as dose rates, temperature effects and method to create disorder are not exactly identical. For instance, with the FPA technique, even though calculations are performed at 300 K, thermal diffusion is prohibited on MD timescales due to the very high migration energies of the defects [34]. The CC calculations were performed at 200 K, preventing long-range defect migration and recombination, and the dose rate was much smaller than in the FPA method. Nevertheless, the most important finding that Fig. 2 points out is that the three disorder accumulation curves exhibit similar features: a rapid increase in the disorder level is observed in the early stage of irradiation, followed by a saturation level at full disorder (i.e. ~100%) that indicates complete amorphization. Therefore, it may be reasonably assumed that the observed discrepancies do not hamper data comparison, providing that a rescaling factor is applied because full amorphization is not reached at the same dpa level for the three cases. The following values were used: 1.15 for FPA, 1.6 for CC and 1 for XRD experiments. The three curves can be fitted with the disorder model above-described (see Eqs.(1-3)). Prior to analysis of the fitting results, it shall be given a few words about how the defect-size distribution depends, in SiC, on both the energy and mass of the PKA. Previous MD results showed that only very small defect clusters (containing typically a few atoms)

are produced in collision cascades created by Si recoils in the keV range [25]; increasing the energy up to 50 keV does not change the defect spectrum since subcascades develop because the maximum stopping power (S_n) of Si in SiC is around 12 keV [35]. This is not the case with heavier recoils, such as 10 keV Au ions which can produce amorphous clusters directly inside a collision cascade [36]. Note that in the present study, $T_{1/2}$ for Si and C recoils during 100 keV Fe irradiation is ~4 keV, a value very close to the 10 keV energy used for the Si PKA in the CC calculations; also, the maximum nuclear stopping of Fe (whose mass is close to that of Si) in SiC is ~35-40 keV. Therefore, from these previous MD results, no direct amorphization is expected, which is indeed what model fits to data indicate since very small values of σ_a are obtained (see Table I). On the contrary, high values of σ_s are observed, indicating, in the framework of the model used here, that amorphization is stimulated. In Fig. 2 are also displayed, for the XRD data, the two contributions to the disorder, namely the amorphous fraction (p_a – dashed line in Fig.2) and the defective fraction (p_c – dash-dotted line in Fig.2). It appears that the former starts to exceed the latter at a dose of ~0.1 dpa. In other words, amorphous regions do form in an appreciable proportion above this dose. This result is consistent with previous MD simulations that clearly showed an increase in size of the defect clusters with increasing dose [25,37]. Yet, both the present FPA analysis and two previous ones, where amorphization of SiC was rendered by accumulation of C displacements only [29,38], indicate that the formation of point defects alone is sufficient to drive the SiC lattice to full amorphization. Therefore, the fact that p_a becomes significant and exceeds p_c from 0.1 dpa necessarily indicates that point defects start to clustering. Moreover, the rapidly growing contribution of p_a strongly suggests that defect clustering is promoted or stimulated. The origin of this stimulation process is addressed in the following. Before that, it is worth mentioning that these results confirm that amorphization in SiC is a homogeneous process consisting in the formation of point defect clusters that grow, thus acting as nuclei for amorphous domains that rapidly expand and eventually lead to the loss of the long-range order.

III.2. Lattice swelling

XRD patterns generated from the simulation cells (both FPA and CC) to obtain the disorder levels have been used to determine the lattice swelling, *i.e.* the relative microscopic volume change. Lattice swelling, which necessarily originates from defective (crystalline) regions only, is related to the relaxation volume of the defects and is directly linked to the lattice strain experimentally measured using XRD [39] (note that it may significantly differ from the macroscopic swelling, which is usually obtained *via* step-height measurements, since this latter is related to the formation volume of the defects). For the CC simulations, an isotropic state of strain was defined and the lattice swelling is directly three times the lattice strain. In the FPA analysis and for the experiments, no in-plane dimensional change is possible and the (anisotropic) lattice strain measured in the out-of-plane direction was first converted into an isotropic strain using a mechanical (elastic) approach that has proven to be relevant in such a situation [27-28]. Note that in this model, elastic constants of the material are required. Two sets of values were used: one derived from the potential used to perform the FPA calculations and another that is an average of experimental values reported in the literature (see [40,41] and references therein). It is worth mentioning that the CC calculations predicted a mechanical softening due to the formation of irradiation defects [42]. However, in order to calculate the isotropic strain, only the ratio of $2C_{12}/C_{11}$ is required (for a (100)-oriented cubic crystal), and this ratio only very weakly changes with irradiation dose [42]. The relevance of such a procedure was tested by comparing the in-plane stress that necessarily develops when no in-plane dimensional change is allowed [27-28]. The stress, compressive since the defect-induced strain is tensile, was found to be -7.5 GPa at 0.1 dpa (i.e. before the stimulation process starts) with both the mechanical model used for the experimental results and the analysis of the FPA data. This perfect agreement validates not only the mechanical model but also the procedure of comparing the swelling obtained from the three different methods.

Figure 3 displays the results of the lattice swelling as a function of the dose. For the entire dose range, and for the three methods, the swelling almost linearly increases with dose. The reason for this finding is that in the present analysis of the lattice swelling, only the crystalline (defective) regions, *i.e.* those which contribute to the XRD peak shift, are considered; the amorphous zones are not taken into account. Therefore, until nearly complete amorphization, the lattice swelling seems to be proportional to the density of introduced defects. Up to a dose of ~0.15 dpa, computational values lie in the error bar of the experimental ones (error bars have been estimated considering the precision of both the measure and the XRD fitting procedure and the uncertainty associated to elastic constants). This result thus shows a reasonable agreement between simulations and experiments up to a dose very close to the end of the amorphization process since, as observed in Fig. 2, the disorder at 0.15 dpa reaches more than 80%. Above this dose, the curves start to separate, and MD predicted values are found to be lower than experimental ones. This discrepancy can be ascribed (i) to a known limitation of the interatomic potential that, as the atomic distances deviate significantly from the perfect crystal, under-predicts the experimentally measured swelling of the amorphous state by about 2 volume % [35], and (ii) to the small number of atoms remaining in the residual crystalline parts of the simulation cells at high irradiation dose. Despite this difference occurring close to the fully amorphous state, the maximum swelling is finally found to be very comparable in magnitude for the three methods, ranging between 4 and 5.5%. This result proves that the MD predictions are valid regarding the relation between atomic-scale crystalline defects and lattice swelling in ion-irradiated SiC. To finish, for the particular case of CC simulations, the maximum lattice swelling is found to be ~5%. In another analysis of the CC simulation data, the total cell swelling was determined and modeled considering that it consists of two contributions: one arising from amorphous regions, and one due to crystalline, defective zones. The maximum contribution to total swelling induced by defective regions only was estimated [37]. A ~6% value was found, in good agreement with the ~5% value

here obtained, which suggests the validity of both the CC calculations and of the procedure in generating XRD patterns from MD cells.

III.3. Defect energy

Now that the link between irradiation defects and swelling is established, the relation between defects (or disorder) and energy should be determined. Such a link has already been established in a previous treatment of the CC simulation data, and a decrease in energy per defect at ~0.1 dpa was determined [18]. In the present work, focus is put on the results obtained by the FPA method, as illustrated in Figure 4, which presents the energy per atom as a function of the dose (symbols). It is observed that there is a rapid and strong energetic destabilization up to 0.1 dpa. Above this dose, where defect clustering leading to formation of amorphous domains starts, the increase in energy is significantly less and slows down. Therefore, the two regimes evidenced in the disordering process are also observed for the variation of the system energy. This observation is in fairly good agreement, even quantitatively, with recent results obtained by MD simulations of C Frenkel pair accumulation in SiC [29]. In order to fit the data of Fig. 4, the disorder model (Eqs. (1-3)) was used with the very same parameters already obtained from the fitting of the disordering kinetics derived from the FPA calculations; in particular, the same amorphization cross-sections, σ_a and σ_s, were used (see Table I). The corresponding curve (solid line in Fig.4) reproduces the computational data, which confirms that disorder and system energy are closely linked. The contribution of defective crystalline regions to the system destabilization was then calculated (dashed line). It clearly appears to be high and preponderant up to a dose of ~0.1 dpa which in fact corresponds to the regime where essentially point defects and very small defect clusters are produced. Therefore, it can be inferred that accumulation of point defects drives the material to a very energetically unstable state and then, a small perturbation, typically a local increase in defect density, triggers the defect clustering and the consequential rapid expansion of

amorphous domains. In other words, the stimulation process occurs to minimize the elastic energy by allowing a defect relaxation when defect clusters grow. Very recently, amorphization of SiC was proposed to be driven by a defect-induced mechanical instability related to the collapse of the (fcc) Si sublattice when the C sublattice is completely disordered. Results obtained in the present work confirm that this instability is indeed mechanical and is related to elastic energy stored into both C and Si defective sublattices when disorder is accumulated. To finish, it is worth mentioning that, even though the lattice swelling is found to be keeping on increasing above 0.15 dpa (see Fig.3), it has little effect on the system energy. This is because in the present analysis of the swelling, the crystalline regions only are considered, and with increasing dose, their volume decreases; in other words, the number of defects that are in amorphous zones increases, and the resulting average cost per defect diminishes, as observed in Fig.4.

IV. Conclusion

To summarize, this study presents a methodology that is based on the same data processing of experimental XRD patterns and XRD patterns generated from MD calculations, in the purpose of evaluating disorder level and lattice swelling in irradiated materials over a large dose range. This methodology, which could be applied to various materials under different irradiation conditions, is here successfully used to study the amorphization process in SiC in the nuclear energy-loss regime. Agreement is obtained between experiments and simulations regarding irradiation-induced disordering and swelling, proving that simulations do reproduce actual atomic-scale processes that occur in irradiated SiC. The interplay between irradiation defects, lattice swelling and defect energy was demonstrated. This allowed showing that amorphization of SiC is a two-step process. In the first step, only point defects or very small defect clusters are produced and they induce a huge lattice swelling, thus a huge elastic energy. In the second step, defect clusters relax towards amorphous domains, and the contribution of defective, highly strained

regions to the energetic destabilization significantly decreases (in other words the stored elastic energy decreases). These amorphous domains that grow at the expense of defective crystalline regions finally lead to complete amorphization.

Acknowledgments

A.D. and A.B. acknowledge the BM02 beamline at ESRF for their help and assistance during HRXRD experiments. F. Gao and W.J. Weber were supported by the U.S. Department of Energy, Office of Basic Energy Sciences, Materials Sciences and Engineering Division. The computational research on collision cascades used resources of the National Energy Research Scientific Computing Center, which is supported by the Office of Science, U.S. Department of Energy under Contract No.DEAC02-05CH11231.

REFERENCES

[1] M. Schulz M., Appl. Phys., 4 (1974) 91.

[2] L. Thomé, J. Jagielski, F. Garrido, Europhys. Lett., 47 (1999) 203.

[3] Y. Katoh, L. L. Snead, I. Szlufarska, W. J. Weber, Current Opinion in Solid State and Materials Science 16 (2012) 143-152.

[4] W. Tang, H. Zhang, Recent Patents on Materials Science 4 (2011) 191.

[5] E. Wendler, A. Heft, W. Wesch, Nucl. Instr. Meth. B 141 (1998) 105.

[6] A. Debelle, L. Thomé, D. Dompoint, A. Boulle, F. Garrido, J. Jagielski, D. Chaussende, J. Phys. D: Appl. Phys. 43 (2010) 455408.

[7] R.S. Averback, Solid State Physics 51 (1997) 281.

[8] A. Chartier, C. Meis, J.-P. Crocombette, L. R. Corrales, W. J. Weber, Phys. Rev. B67 (2003) 174102.

[9] J. Lian, X. T. Zu, K. V. G. Kutty, J. Chen, L. M. Wang, and R. C. Ewing, Phys. Rev. B. 66 (2002) 054108.

[10] S. Moll, G. Sattonnay, L. Thomé, J. Jagielski, C. Decorse, P. Simon, I. Monnet, W. J. Weber, Phys. Rev. B. 84 (2011) 064115.

[11] K. Trachenko, J. Phys.: Condens. Matter 16 (2004) R1491.

[12] W.J. Weber, Nucl. Instrum. Meth. B 166-167 (2000) 98.

[13] Y. Zhang, W.J. Weber, W. Jiang, C.M. Wang, V. Shutthanandan, A. Hallen, J. Appl. Phys. 95 (2004) 4012.

[14] W. Jiang, Y. Zhang, W. J. Weber, Phys. Rev. B 70 (2004) 165208.

[15] S. Sorieul, J.-M. Costantini, L. Gosmain, L.Thomé, J.-J. Grob, J. Phys.: Condens. Matter 18 (2006) 5235.

[16] Z. Zolnai, A. Ster, N.Q. Khanh, G. Battistig, T. Lohner, J. Gyulai, E. Kotai, M. Posselt, J. Appl. Phys. 101 (2007) 023502.

[17] A. Debelle, M. Backman, L. Thomé, K. Nordlund, F. Djurabekova, W.J. Weber, I. Monnet, O.H. Pakarinen, F. Garrido, F. Paumier, Nucl. Instr. Meth. B 326 (2014) 326.

[18] W.J. Weber, F. Gao, J. Materials Research 25 (2010) 2349.

[19] J.F. Ziegler, J. P. Biersack, U. Littmark, The Stopping and Range of Ions in Solids, Pergamon, New York, 1985. Available at: www.srim.org.

[20] R. Devanathan, W. J. Weber, F. Gao, J. Appl. Phys. 90 (2001) 2303.

[21] G. Lucas, L. Pizzagalli, Phys. Rev. B 72 (2005) 161202.

[22] R.S. Averback, J. Nucl. Mater. 216 (1994) 49.

[23] A Boulle, R Guinebretière, A Dauger, J. Phys. D: Appl. Phys. 38 (2005) 3907.

[24] A. Boulle, A. Debelle, J. Appl. Cryst. 43 (2010) 1046.

[25] F. Gao, W.J. Weber, Physical Review B 66 (2002) 024106.

[26] S.I. Rao, C.R. Houska, J. Mater. Science 25 (1990) 2822.

[27] A. Debelle, A. Declémy, Nucl. Instr. and Meth. B 268 (2010) 1460.

[28] A. Debelle, A. Boulle, F. Rakotovao, J. Moeyaert, C. Bachelet, F. Garrido, L. Thomé, J. Phys. D: Appl. Phys. 46 (2013) 045309.

[29] C. Jiang, M.-J. Zheng, D. Morgan, I. Szlufarska, Phy. Rev. Lett. 111 (2013) 155501.

[30] A. Chartier, C. Meis, J.-P. Crocombette, W.J. Weber, L.R. Corrales, Phys. Rev. Lett. 94 (2005) 025505.

[31] J.-P. Crocombette, A. Chartier, W. J. Weber, Appl. Phys. Lett. 88 (2006) 051912.

[32] K. Nordlund, U. Beck, T.H. Metzger, J.R. Patel, Appl. Phys. Lett. 76 (2000) 846.

[33] Y.H. Li, B.P. Uberuaga, C. Jiang, S. Choudhury, J.A. Valdez, M.K. Patel et al., Phys. Rev. Lett. 108 (2012) 195504.

[34] F. Gao, G. Henkelman, W. J. Weber, L. R. Corrales, H. Jonsson, Nuclear Instruments and Methods in Physics Research B 202 (2003) 1.

[35] F. Gao, W.J. Weber, Phys. Rev. B 63 (2000) 054101.

[36] F. Gao, W. J. Weber, J. Appl. Phys. 89 (2001) 4275.

[37] F. Gao and W.J. Weber, J. Mater Res., 18 (2003) 1877.

[38] R. Devanathan, F. Gao, W.J. Weber, Appl. Phys. Lett. 84 (2004) 3909.

[39] P. Ehrhart, J. Nucl. Mater. 216 (1994) 170.

[40] W.R.L. Lambrecht, B. Segall, M. Methfessel, M. van Schilfgaarde, Phys. Rev. B. 44 (1991) 3685.

[41] K.A. Pestka, II, J.D. Maynard, D. Gao, C. Carraro, Phys. Rev. Lett. 100 (2008) 055503.

[42] F. Gao, W.J. Weber, Phys. Rev. B 69 (2004) 224108.

Table caption

Cross-section values of direct (σ_a) and stimulated (σ_s) amorphization obtained from the fitting of FPA and CC computational data and of experimental XRD data presented in Fig.2.

	FPA	CC	Exp. XRD
σ_a (dpa^{-1})	0.4	4	1
σ_s (dpa^{-1})	28	32	25

FIGURE CAPTIONS

Figure 1: HRXRD measurements (thick lines) of the (004) reflection of virgin and irradiated 3C-SiC. Labels correspond to the ion doses expressed in dpa. Curves are shifted vertically for visualization purposes. Simulations of experimental curves are plotted as thin lines. Corresponding strain depth profiles are displayed in inset; dotted lines correspond to regions where SiC is fully amorphized, and therefore the swelling information is irrelevant.

Figure 2: Relative disorder as a function of damage expressed in dpa in irradiated SiC obtained from MD simulations and XRD experiments. The dashed and dash-dotted lines correspond to p_a and p_c fractions for the experimental disorder, respectively.

Figure 3: Lattice swelling (microscopic volume change) in MD cells and real SiC crystals as a function of the damage expressed in dpa.

Figure 4: Energy per atom, derived from the FPA technique, as a function of the damage expressed in dpa (symbols). The solid line corresponds to best-fit with the presented disorder model (see text). The dashed line illustrates the contribution to the increase in energy due to defective, crystalline regions.

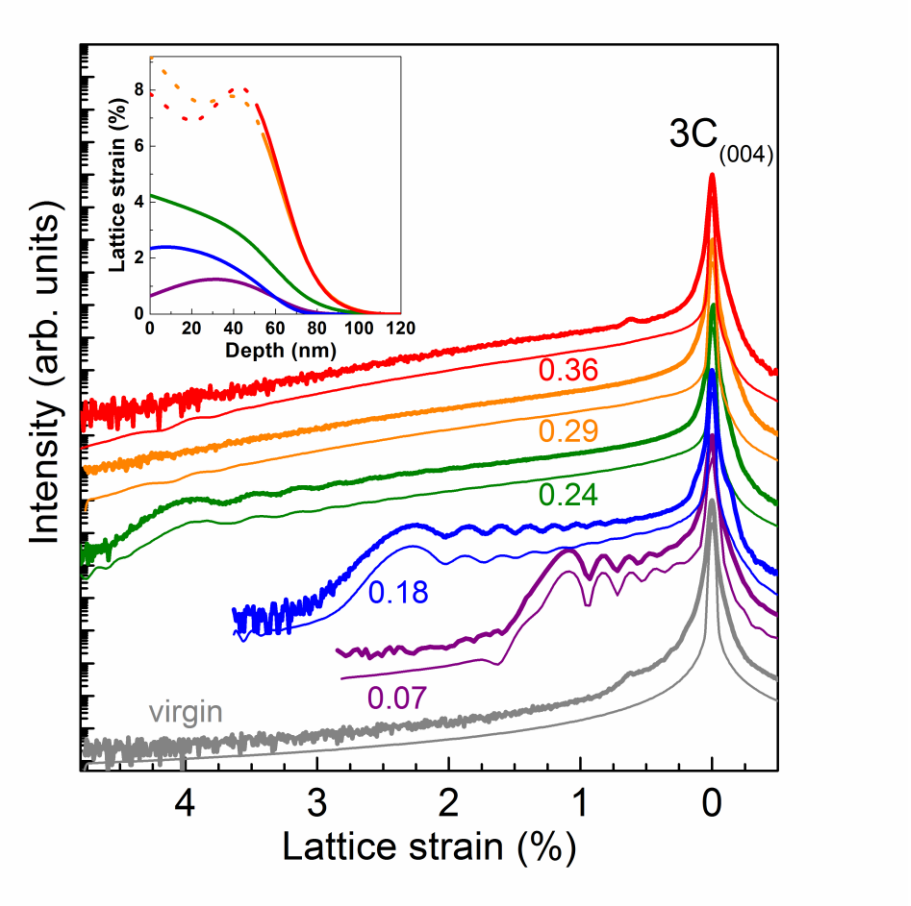
Intensity (arb. units)
Lattice strain (%)
Depth (nm)
Lattice strain (%)
3C(004)
0.36
0.29
0.24
0.18
0.07
virgin

FIGURE 1

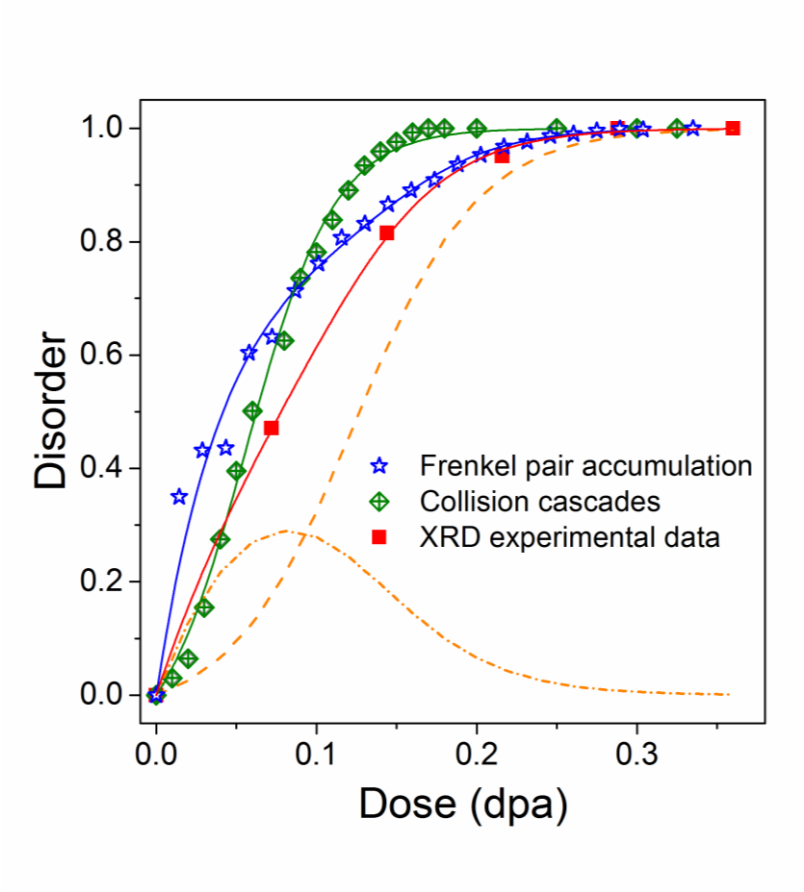
Disorder
Dose (dpa)
1.0
0.8
0.6
0.4
0.2
0.0
0.0
0.1
0.2
0.3
Frenkel pair accumulation
Collision cascades
XRD experimental data

FIGURE 2

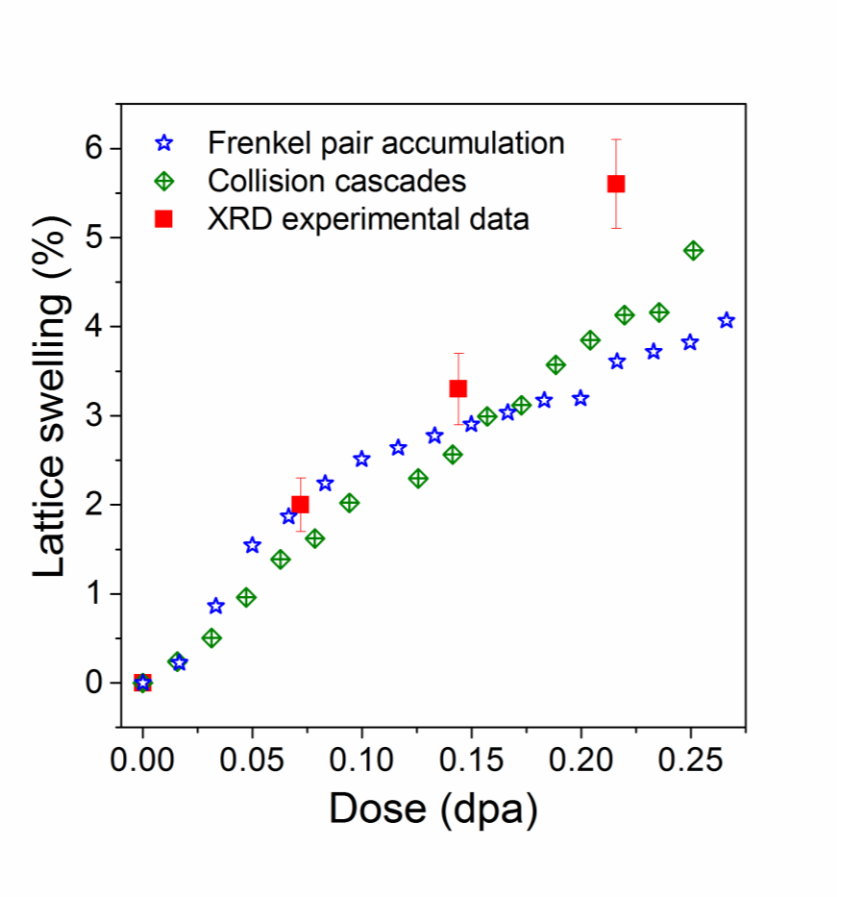
Frenkel pair accumulation
Collision cascades
XRD experimental data
Lattice swelling (%)
Dose (dpa)
0
1
2
3
4
5
6
0.00
0.05
0.10
0.15
0.20
0.25

FIGURE 3

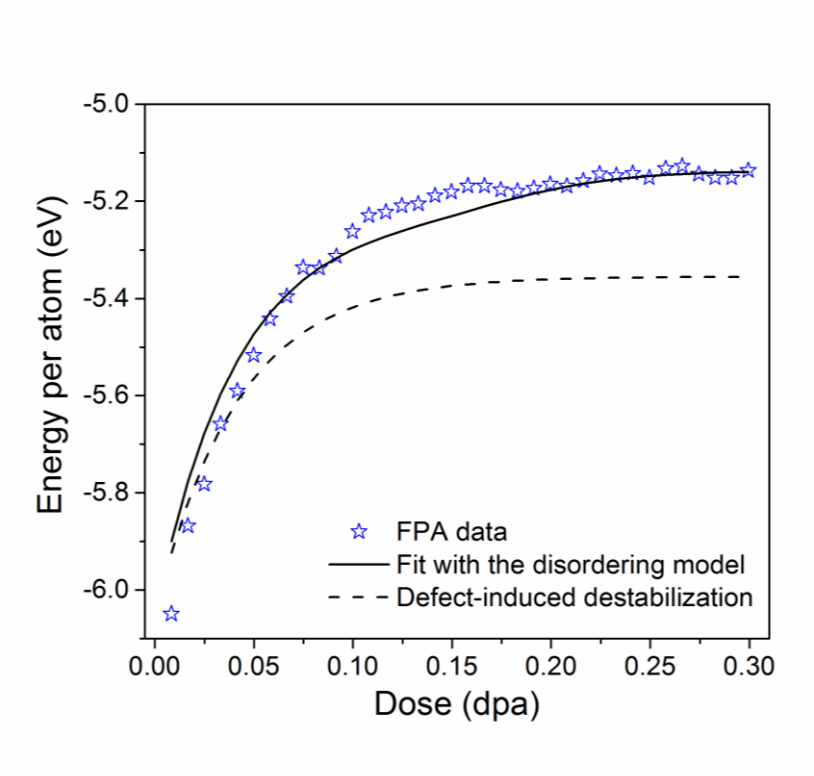
-5.0
-5.2
-5.4
-5.6
-5.8
-6.0
Energy per atom (eV)
0.00
0.05
0.10
0.15
0.20
0.25
0.30
Dose (dpa)
FPA data
Fit with the disordering model
Defect-induced destabilization

FIGURE 4